Quantum-Squeezing-Induced Point-Gap Topology and Skin Effect

Liang-Liang Wan and Xin-You Lü*
School of Physics and Institute for Quantum Science and Engineering, Huzhong University of Science and Technology, Wuhan 430074, China and Wuhan Institute of Quantum Technology, Wuhan 430074, China

(Received 17 November 2022; accepted 21 April 2023; published 19 May 2023)

We theoretically predict the squeezing-induced point-gap topology together with a symmetry-protected $\mathbb{Z}_2$ "skin effect" in a one-dimensional (1D) quadratic-bosonic system. Protected by a time-reversal symmetry, such a topology is associated with a novel $\mathbb{Z}_2$ invariant (similar to quantum spin-Hall insulators), which is fully capable of characterizing the occurrence of the $\mathbb{Z}_2$ skin effect. Focusing on zero energy, the parameter regime of this skin effect in the phase diagram just corresponds to a "real- and point-gap coexisting topological phase." Moreover, this phase associated with the symmetry-protected $\mathbb{Z}_2$ skin effect is experimentally observable by detecting the steady-state power spectral density. Our Letter is of fundamental interest in enriching non-Bloch topological physics by introducing quantum squeezing and has potential applications for the engineering of symmetry-protected sensors based on the $\mathbb{Z}_2$ skin effect.

DOI: 10.1103/PhysRevLett.130.203605

The concept of topological phases of matter has radiated from condensed-matter physics to several fields including photonics [1], magnetoplasmon [2], mechanics [3–6], cold atoms [7,8], metasurface [9–11], etc. In particular, growing efforts are paid to search for distinctive topological phenomena in non-Hermitian systems [12–43]. The most intriguing is the non-Hermitian skin effect [14,18], which refers to the localization of bulk states at boundaries. Accompanied with the breakdown of the bulk-boundary correspondence, it stems from the point-gap topology where the complex-valued spectrum enclosing an energy point has a nonvanishing winding number [19,22–24,30,31].

Squeezing of bosonic fields [44], as a useful technique of quantum engineering, could not only exponentially enhance light-matter interactions [45–52], but also induce instability of edge states in quadratic-bosonic systems (QBSs) [53–57]. In the sense that the instability arises from the complex-valued spectrum given by a non-Hermitian matrix, the QBS is also of interest in the framework of non-Hermitian physics [58,59]. The topological classification for the generic QBS is established based on the Bernard-LeClair 38-fold symmetry classes [60], and it predicts the topological triviality of 1D QBS in terms of zero energy [23]. However, the bosonic Kitaev chain exhibits an end-to-end amplification and has the analog of Majorana zero modes [61–66], which should be an effect of point-gap topology. Such a contradiction implies that the topological nature of QBSs still remains unclear, and solving this contradiction is fundamentally interesting in exploring the exotic topological phenomena (e.g., skin effect).

Here, we investigate the topological origin of a 1D QBS in the thermodynamic-instability regime. By introducing an unconventional time-reversal symmetry, we discover that the squeezing can induce the appearance of point-gap topology together with a symmetry-protected $\mathbb{Z}_2$ skin effect in the QBS. The mechanism relies on additional symmetry enriching the topology of system. In contrast to the imaginary gauge transformation in non-Hermitian systems [18,24,26,67,68], this skin effect corresponds to a real squeezing transformation, and it is extremely sensitive to the local perturbation that breaks the time-reversal symmetry of system. By increasing the squeezing until the point gap is open at zero energy, we also find the survival of a pair of zero modes in the open boundary condition (OBC) even if the real gap closes in the periodic boundary condition (PBC). This indicates an anomalous bulk-boundary correspondence and the appearance of a real- and point-gap coexisting topological phase. Meanwhile, the $\mathbb{Z}_2$ skin effect, appearing in this coexisting phase, inhibits another pair of zero modes.

Compared with the previous works focusing on the transport amplification [61,62,65], Majorana bosonic analogs together with the topological metastability [63,64], and non-Bloch wave behaviors [69], here we introduce an unconventional time-reversal symmetry to the QBS and uncover the symmetry-enriched topological classification. Remarkably, we also find the real- and point-gap coexisting topological phase, and it can be identified by the steady-state power spectral density. Our Letter builds the connection between point-gap topology together with skin effect and quantum squeezing. It opens up a door for exploring the crossover between topological physics and quantum engineering and offers potential applications in designing new types of topological-protected devices.

Squeezing-induced point-gap topology.—Let us consider a 1D QBS subject to the lattice-translational symmetry with Hamiltonian $\hat{H} = \frac{1}{2}\sum_k \hat{\Phi}_k^\dagger H(k)\hat{\Phi}_k$. Here $H(k)$ is the first-quantized Hamiltonian of the QBS in the crystal-momentum space, and $\hat{\Phi}_k = (\hat{a}_{k1}, \ldots, \hat{a}_{kN}, \hat{a}_{-k1}^\dagger, \ldots, \hat{a}_{-kN}^\dagger)^T$ is the Nambu spinor in terms of $2N$ bosonic annihilation and creation operators with k and $-k$, respectively. The spinor obeys $[\hat{\Phi}_{ki}, \hat{\Phi}_{k'j}^\dagger] = \delta_{kk'}(\tau^3)_{ij}$, with τ^3 being the indefinite metric [70,71]. Here, $\tau^i = \sigma^i \otimes I_N$ with the Pauli matrices σ^i $(i = 1, 2, 3)$. The system dynamics is described by $(\partial/\partial t)\hat{\Phi}_k(t) = -iH_\tau(k)\hat{\Phi}_k(t)$, with $H_\tau(k) = \tau^3 H(k)$ being non-Hermitian. The dynamical matrix $H_\tau(k)$ inherently respects the particle-hole symmetry $\mathcal{C}H_\tau^*(-k)\mathcal{C}^{-1} = -H_\tau(k)$, with $\mathcal{C} = \tau^1$ being the "charge conjugation" [72–74] and the pseudo-Hermiticity $\eta H_\tau^\dagger(k)\eta^{-1} = H_\tau(k)$, with $\eta = \tau^3$ [75].

In the thermodynamic-instability regime, the squeezing may induce a complex-valued spectrum formed by loops in the PBC and open curves in the OBC [61,62,76]. This scenario is a reminiscence of the point-gap topology in non-Hermitian systems [19,22,23]. In terms of zero energy, we construct the Hermitian matrix

$$\tilde{H}_\tau(k) = \begin{pmatrix} 0 & H_\tau(k) \\ H_\tau^\dagger(k) & 0 \end{pmatrix}, \tag{1}$$

which respects the chiral symmetry $\Gamma\tilde{H}_\tau\Gamma^{-1} = -\tilde{H}_\tau$, with $\Gamma = I_{2N} \oplus -I_{2N}$. This symmetry leads to the winding number $W \in \mathbb{Z}$ given by

$$W = \int_{\mathrm{BZ}} \frac{dk}{2\pi i}\frac{\partial}{\partial k}\ln\det H_\tau(k). \tag{2}$$

Equation (2) is always trivial due to the pseudo-Hermiticity. However, in general, the symmetry class together with the topological classification for the QBS would be altered once some additional symmetries are introduced. Hence, the presence of additional symmetries can enrich the topological phase of the QBS (see Supplemental Material [77]).

For illustration, we study the squeezed Su-Schrieffer-Heeger (SSH) model shown in Fig. 1(a). The system Hamiltonian is

$$\hat{H}_{\mathrm{SSH}} = \sum_{j\in\mathbb{Z}}(t_1\hat{a}_{j,A}^\dagger\hat{a}_{j,B} + t_2\hat{a}_{j+1,A}^\dagger\hat{a}_{j,B} + g_1\hat{a}_{j,A}\hat{a}_{j,B} + g_2\hat{a}_{j+1,A}\hat{a}_{j,B} + \mathrm{H.c.}), \tag{3}$$

where t_1, $t_2 > 0$ are the hopping strengths between the nearest-neighbor sites, and $g_1, g_2 \in \mathbb{R}$ are the strengths of the intra- and intercell squeezing, respectively. This model can be implemented in many platforms, such as quantum superconducting circuits [86–90] and photonic crystals with optomechanical interaction [91–93]. In particular, the crucial bosonic squeezing can be implemented via the three-wave mixing process introduced by the Josephson ring modulator or superconducting nonlinear asymmetric inductive element device [77].

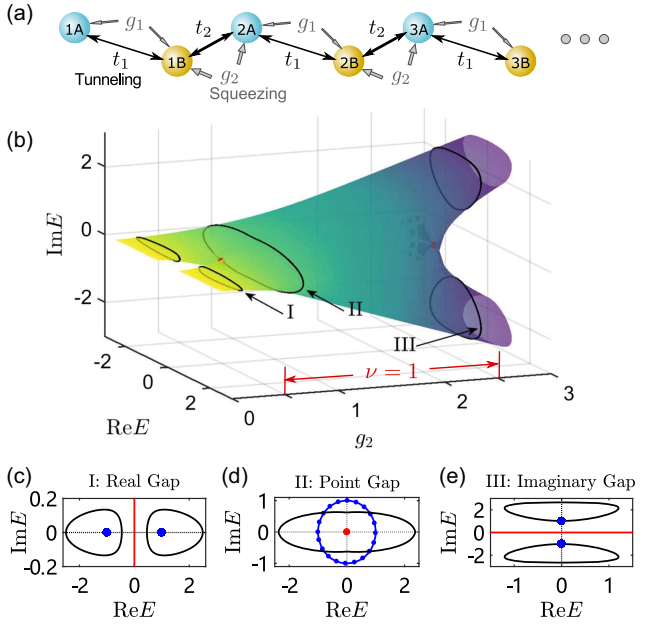

FIG. 1. (a) Schematic of the squeezed SSH model consisting of the A and B sublattices in the presence of two-mode squeezing. The hopping and squeezing strengths between the adjacent sites are denoted by t_1, t_2 and g_1, g_2, respectively. (b) Spectrum in the complex plane as varying the intercell squeezing strength g_2. Here $t_2 = 3t_1/2$ and $g_1 = 0$. The red dots at $g_2 = 0.5t_1, 2.5t_1$ represent the critical points for closing or opening the point gap at $E = 0$, and $\nu = 1$ corresponds to $g_2 \in (0.5, 2.5)t_1$. (c)–(e) Spectra (black curves) for I, II, and III in (b) can be continuously deformed to (c) ± 1 (blue dots), (d) unit circle (blue circle), and (e) $\pm i$ (blue dots), respectively, while preserving the associated gaps (red).

The Bloch spectrum with a twofold degeneracy is $E_\pm^2(k) = \Delta^2 + 2(t_1t_2 - g_1g_2)\cos k \pm 2i(t_1g_2 - t_2g_1)\sin k$, with $\Delta = \sqrt{t_1^2 + t_2^2 - g_1^2 - g_2^2}$. Figures 1(b)–1(e) show that the spectrum experiences three processes in the complex plane as increasing g_2. First, two isolated loops are located at the real axis (I) and, subsequently, a curve encloses zero energy (II). Finally, two isolated loops move to the imaginary axis (III). Those processes have the real ($\mathrm{Re}E = 0$), point ($E = 0$), and imaginary ($\mathrm{Im}E = 0$) gaps, respectively. This hints at the appearance of nontrivial point-gap topology at zero energy in regime II induced by squeezing.

Specifically, the winding number (2) for our system is trivial, when the Bogoliubov bands enclose zero energy shown in Figs. 1(b) and 1(d). However, the system also respects a sublattice symmetry $\mathcal{S}H_{\tau\mathrm{SSH}}(k)\mathcal{S}^{-1} = -H_{\tau\mathrm{SSH}}(k)$, with $\mathcal{S} = \sigma^3$ being the sublattice and $H_{\tau\mathrm{SSH}}$

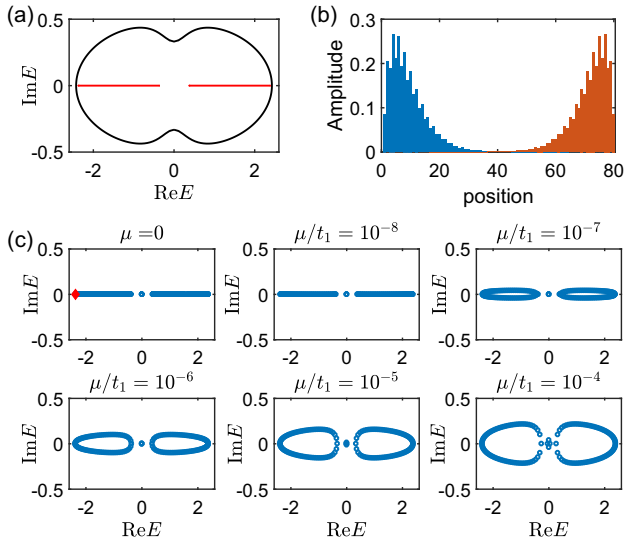

FIG. 2. (a) Spectrum (black) of the squeezed SSH model under the PBC and the corresponding continuum bands (red) after the mapping (6). (b) Amplitudes of the Kramers pair with the lowest energy (blue and red bars) for both the particles and holes in the OBC. The localization of the two degenerate states manifests the $\mathbb{Z}_2$ skin effect. (c) Spectra of the perturbed model in the OBC with varying the chemical potential $\mu = (0, 10^{-8}, 10^{-7}, 10^{-6}, 10^{-5}, 10^{-4})t_1$. The red diamond mark denotes the Kramers pair in (b). Parameters: $t_2 = 1.5t_1$, $g_1 = 0$, $g_2 = 0.6t_1$, and $L = 40$.

being the dynamical matrix. The combination of the particle-hole symmetry, pseudo-Hermiticity, and sublattice symmetry yields an unconventional time-reversal symmetry [13,94,95],

$$\mathcal{T} H^T_{\tau\mathrm{SSH}}(-k)\mathcal{T}^{-1} = H_{\tau\mathrm{SSH}}(k), \quad \mathcal{T}\mathcal{T}^* = -I, \tag{4}$$

with $\mathcal{T} = i\tau^2\sigma^3$. In terms of zero energy, this symmetry supports a $\mathbb{Z}_2$ invariant $\nu \in \{0, 1\}$, defined by [23,77]

$$(-1)^\nu = \mathrm{sgn}\left[\frac{\mathrm{Pf}[H_{\tau\mathrm{SSH}}(0)\mathcal{T}]}{\mathrm{Pf}[H_{\tau\mathrm{SSH}}(\pi)\mathcal{T}]}\right], \tag{5}$$

where $\mathrm{Pf}(O)$ denotes the Pfaffian for any skew-symmetric matrix O ($O^T = -O$). This $\mathbb{Z}_2$ invariant gives the critical points at $|t_1 \pm t_2| = |g_1 \pm g_2|$, i.e., the red dots in Fig. 1(b), which shows a squeezing-induced nontrivial point-gap topology in regime II. Moreover, in regimes I and III, the point-gap topology of the system can also be nontrivial, if the reference energy E is not zero and is placed in the closed loop [77].

Symmetry-protected $\mathbb{Z}_2$ skin effect.—In the presence of point-gap topology, the spectrum of the Hamiltonian (3) dramatically changes from a closed curve [black loop in Fig. 2(a)] to the discrete points that form open lines [see the first panel of Fig. 2(c)] under the OBC. Consequently, as shown in Fig. 2(b), the Kramers pair guaranteed by the time-reversal symmetry (4) is localized at both ends, which shows the appearance of the symmetry-protected $\mathbb{Z}_2$ skin effect [30,96,97].

In general, the non-Hermitian skin effect corresponds to an imaginary gauge transformation [18,24,26,67,68]. However, here the $\mathbb{Z}_2$ skin effect corresponds to a real squeezing transformation with operator $\hat{S}$ [77]. Specifically, under the parameter condition of $g_1 = 0$ and $t_2 > |g_2|$, we perform a squeezing transformation to the "particles" $\hat{a}_{j\sigma}$ and "holes" $\hat{a}^\dagger_{j\sigma}$ with $\sigma = A, B$ such that

$$\begin{pmatrix} \hat{a}_{j,A/B} \\ \hat{a}^\dagger_{j,A/B} \end{pmatrix} = (e^{\pm r\tau^1})^j \begin{pmatrix} \hat{\alpha}_{j,A/B} \\ \hat{\alpha}^\dagger_{j,A/B} \end{pmatrix}. \tag{6}$$

Here the squeezing parameter r satisfies $\tanh r = -g_2/t_2$. The squeezing transformation (6) inherently belongs to SU(1,1) [98], and the particles and holes $(\hat{\alpha}_{j\sigma}, \hat{\alpha}^\dagger_{j\sigma})$ in the new quasiparticle basis preserve $[\hat{\alpha}_{j\sigma}, \hat{\alpha}^\dagger_{j'\sigma'}] = \delta_{jj'}\delta_{\sigma\sigma'}$. Using this transformation (6), the Hamiltonian (3) is mapped to the conventional SSH model with Hamiltonian $\hat{H}_{\mathrm{SSH}} = \sum_{j=1}^{L} t_1\hat{\alpha}^\dagger_{jA}\hat{\alpha}_{jB} + \tilde{t}_2\hat{\alpha}^\dagger_{j+1A}\hat{\alpha}_{jB} + \mathrm{H.c.}$, where $\tilde{t}_2 = \sqrt{t_2^2 - g_2^2}$ and L is the number of the total unit cells. As shown in Fig. 2(a), the spectrum of $\hat{H}_{\mathrm{SSH}}$ becomes two open (red) lines in the continuum limit $L \to \infty$ corresponding to the PBC [99], which indicates the disappearance of the skin effect in the squeezed-state representation. This demonstrates that the obtained $\mathbb{Z}_2$ skin effect originally comes from the intercell squeezing $\sum_j g_2(\hat{a}_{jB}\hat{a}_{j+1A} + \mathrm{H.c.})$ in the QBS.

Physically, such squeezing interaction describes a nondegenerate parametric amplification process and gives rise to the entanglement between two bosonic modes in the adjacent unit cells. Then, the introduced intercell parametric amplification in the 1D lattice induces intrinsically the non-Hermiticity of the system, which ultimately leads to the appearance of the point-gap topology together with the symmetry-protected $\mathbb{Z}_2$ skin effect (see Supplemental Material [77]).

This $\mathbb{Z}_2$ skin effect is extremely sensitive against local symmetry-breaking perturbations [26,77,97]. To show this, we introduce an on-site perturbation $\hat{H}_{\text{on site}} = \mu\sum_{j\sigma}\hat{a}^\dagger_{j\sigma}\hat{a}_{j\sigma}$ to the system, which breaks the time-reversal symmetry (4). Applying the squeezing transformation (6) to the perturbation, we obtain

$$\hat{H}_{\text{on site}} = \mu\sum_{j=1}^{L}\Big[\cosh(2rj)(\hat{\alpha}^\dagger_{jA}\hat{\alpha}_{jA} + \hat{\alpha}^\dagger_{jB}\hat{\alpha}_{jB}) + \frac{\sinh(2rj)}{2}(\hat{\alpha}^\dagger_{jA}\hat{\alpha}^\dagger_{jA} - \hat{\alpha}^\dagger_{jB}\hat{\alpha}^\dagger_{jB} + \mathrm{H.c.})\Big]. \tag{7}$$

The impact of Eq. (7) on the unperturbed Hamiltonian is qualitatively determined by the scaling [26,69,101]

$$\mu/t_1 \sim e^{-|r|L}. \tag{8}$$

It implies that the presence of an infinitesimal perturbation also can change the physics of the system in the continuum limit. Such an instability arises from the breakdown of the time-reversal symmetry. More precisely, the anomalous squeezing in (7) dramatically alters the spectrum by coupling the Kramers pairs localized at the opposite ends of the chain [see Fig. 2(b)]. As shown in Fig. 2(c), the instability of the spectrum occurring at $\mu/t_1 \sim 10^{-8}$ confirms our analysis.

Real- and point-gap coexisting topological phase.—The parameter regime of $\mathbb{Z}_2$ skin effect actually corresponds to a real- and point-gap coexisting topological phase due to the interplay between the squeezing and particle-exchange coupling. Such a phase is unconventional since the real gap is closed in the PBC, while the zero mode survives in the OBC, which indicates an anomalous bulk-boundary correspondence. Meanwhile, the point-gap topology is also nontrivial. To show this, in Fig. 3, we plot the phase diagram for the real-gap topology by calculating the winding number in the PBC and the zero modes in the OBC.

First, the real gap $\mathrm{Re}E = 0$ opens in the PBC if $|g_2| < |t_2 - t_1|$ holds, as shown in Fig. 1(b). Because of the sublattice symmetry $\mathcal{S}$, the real-gap topology can be characterized by the winding number $W^{(\mathrm{real})} = (1/2\pi i)\int_{\mathrm{BZ}} q^{-1}dq$, with $q = t_1 + t_2 e^{ik}$ [77]. This winding number is nontrivial for $t_1 + |g_2| < t_2$, corresponding to the yellow area of Fig. 3. The bulk-boundary correspondence ensures the emergence of zero modes in the bulk gap. In the

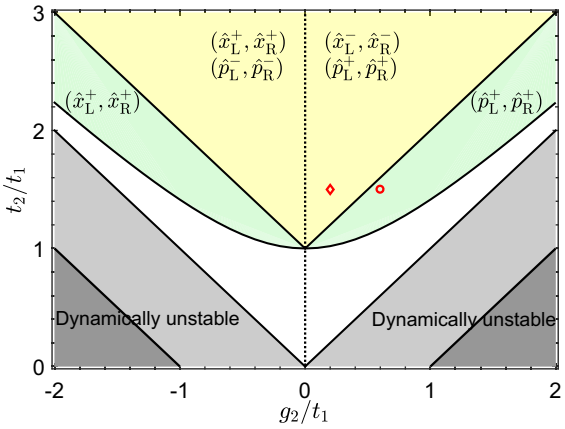

FIG. 3. Phase diagram of the 1D QBS for $g_1 = 0$. In the yellow area, the real gap opens in the PBC, and two pairs of zero modes $(\hat{x}_{\mathsf{L}}^{\pm}, \hat{x}_{\mathsf{R}}^{\pm})$ and $(\hat{p}_{\mathsf{L}}^{\mp}, \hat{p}_{\mathsf{R}}^{\mp})$ appear in the OBC. The green area indicates a real- and point-gap coexisting topological phase with a zero-mode pair. The dark gray areas correspond to the imaginary-gap topological phase. The system has no zero mode in the white area and is dynamically unstable in the light and dark gray areas under the OBC.

representation of the canonical coordinates and momenta $\hat{x}_{j\sigma} = (\hat{a}_{j\sigma} + \hat{a}_{j\sigma}^{\dagger})/\sqrt{2}$ and $\hat{p}_{j\sigma} = (\hat{a}_{j\sigma} - \hat{a}_{j\sigma}^{\dagger})/\sqrt{2}i$, two pairs of zero modes $\hat{x}_{\mathsf{L}}^{-s} = \sum_{j=1}^{L} \delta_{-s}^{j-1}\hat{x}_{jA}$, $\hat{x}_{\mathsf{R}}^{-s} = \sum_{j=1}^{L} \delta_{-s}^{L-j}\hat{x}_{jB}$ and $\hat{p}_{\mathsf{L}}^{s} = \sum_{j=1}^{L} \delta_{s}^{j-1}\hat{p}_{jA}$, $\hat{p}_{\mathsf{R}}^{s} = \sum_{j=1}^{L} \delta_{s}^{L-j}\hat{p}_{jB}$, with $\delta_{\pm s} = -t_1/(t_2 \pm s|g_2|)$ and $s = \mathrm{sgn}(g_2) = \pm(|\delta_{\pm}| < 1)$ appear in the OBC [77]. Here the subscripts L and R denote the left and right edges of the 1D QBS, respectively. $[\hat{x}_{\mathsf{L}}^{-s}, \hat{p}_{\mathsf{L}}^{s}] = [\hat{x}_{\mathsf{R}}^{-s}, \hat{p}_{\mathsf{R}}^{s}] = i(1-\delta^{2L})/(1-\delta^2)$ $(\delta = -t_1/\tilde{t}_2)$ implies that $\hat{x}_{\mathsf{L/R}}^{-s}$ and $\hat{p}_{\mathsf{L/R}}^{s}$ are canonically conjugate with each other.

As increasing g_2, the real gap closes at $t_1 + |g_2| = t_2$, while a pair of zero modes $(\hat{x}_{\mathsf{L}}^{+}, \hat{x}_{\mathsf{R}}^{+})$ or $(\hat{p}_{\mathsf{L}}^{+}, \hat{p}_{\mathsf{R}}^{+})$ can survive. This means that the conventional bulk-boundary correspondence based on $W^{(\mathrm{real})}$ is no longer valid. To reconstruct it, we impose the continuum limit to the mapped Hamiltonian $\hat{H}_{\mathrm{SSH}}$ and find that the real gap preserves in the region $|g_2| < t_2$ under the PBC. Furthermore, the reconstructed winding number $\tilde{W}^{(\mathrm{real})}$ [77] indicates the new nontrivial phase (i.e., $\sqrt{t_1^2 + g_2^2} < t_2$), corresponding to the yellow and green areas of Fig. 3.

In terms of $E = 0$, the defined ν is nontrivial in the green area, which indicates a real- and point-gap coexisting topological phase. Correspondingly, the symmetry-protected $\mathbb{Z}_2$ skin effect appears and greatly inhibits the occurrence of a pair of zero modes, either $(\hat{x}_{\mathsf{L}}^{-}, \hat{x}_{\mathsf{R}}^{-})$ for $g_2 > 0$ or $(\hat{p}_{\mathsf{L}}^{-}, \hat{p}_{\mathsf{R}}^{-})$ for $g_2 < 0$. This inhibition originates from the localization competition between the skin effect and zero modes of the conventional SSH model [77]. Meanwhile, another pair of zero modes $(\hat{p}_{\mathsf{L}}^{+}, \hat{p}_{\mathsf{R}}^{+})$ or $(\hat{x}_{\mathsf{L}}^{+}, \hat{x}_{\mathsf{R}}^{+})$ survive, and they are extremely sensitive to the local perturbation (7). The scaling of μ can be heuristically estimated by $\mu/t_1 \sim \xi^{-L}$, with $\xi = e^{|r|}|\delta|^{1/2}$. Figure 2(c) shows that the zero modes $(\hat{p}_{\mathsf{L}}^{+}, \hat{p}_{\mathsf{R}}^{+})$ almost disappear at $\mu/t_1 \sim 3 \times 10^{-5}$, which is consistent with this critical scaling. As continuously increasing g_2, the imaginary gap is open and the associated topology becomes nontrivial in regime III of Figs. 1(b) and 1(e), corresponding to the dark gray areas of Fig. 3. Moreover, the phase diagram can be enriched further when the intracell squeezing is introduced, i.e., $g_1 \neq 0$ [77].

Detection of the coexisting topological phase together with the $\mathbb{Z}_2$ skin effect.—For detection, we calculate the normalized power spectral density $S_{\rho_{j\sigma}\rho_{j\sigma}}(\omega) = \int d\tau \langle \hat{\rho}_{j\sigma}(\tau)\hat{\rho}_{j\sigma}(0)\rangle_{\mathrm{ss}} e^{i\omega\tau}/\langle \hat{\rho}_{j\sigma}(0)\hat{\rho}_{j\sigma}(0)\rangle_{\mathrm{ss}}$ in the presence of decay with rate γ [77]. Here $\langle\cdot\rangle_{\mathrm{ss}}$ denotes a steady-state expectation value and $\hat{\rho}_{j\sigma} = \hat{x}_{j\sigma}, \hat{p}_{j\sigma}$. Normally, any zero mode corresponds to the peak of $|S_{\rho_{j\sigma}\rho_{j\sigma}}(0)|$ at edge sites. Focusing on the first site 1A, the zero modes $\hat{x}_{\mathsf{L}}^{-s}$ and $\hat{p}_{\mathsf{L}}^{s}$ correspond to the peaks of $|S_{x_{1A}x_{1A}}(0)|$ and $|S_{p_{1A}p_{1A}}(0)|$, respectively. Then double peaks at zero frequency in Fig. 4(a) indicate the real-gap topological phase (yellow area of Fig. 3), and one peak in Fig. 4(b) depicts the

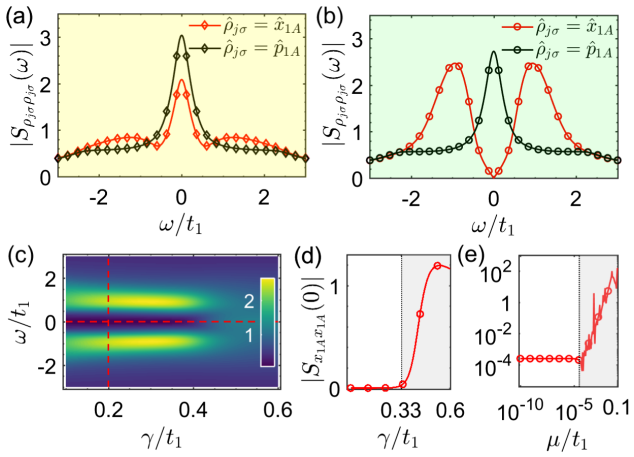

FIG. 4. (a),(b) Power spectral density $|S_{\rho_{j\sigma}\rho_{j\sigma}}(\omega)|$, with $\hat{\rho}_{j\sigma} = \hat{x}_{1A}, \hat{p}_{1A}$ versus ω when $\gamma = 0.2t_1$, (a) $g_2 = 0.2t_1$ and (b) $g_2 = 0.6t_1$, corresponding to the diamond and circle in Fig. 3. (c) $|S_{x_{1A}x_{1A}}(\omega)|$ as varying γ and ω. The red dashed lines denote the cases in (b) and (d), respectively. (d) $|S_{x_{1A}x_{1A}}(0)|$ versus γ. The zero-frequency dip vanishes at the critical decay $\gamma_c \approx 0.33t_1$. (e) $|S_{x_{1A}x_{1A}}(0)|$ versus μ when $\gamma = 0.2t_1$. The topological inhibition vanishes at $\mu/t_1 \sim 3 \times 10^{-5}$. Parameters: $t_2 = 1.5t_1$, $g_1 = 0$, $L = 40$, and (c)–(e) $g_2 = 0.6t_1$.

real- and point-gap coexisting topological phase (green area in Fig. 3). Moreover, the peaks of $|S_{x_{1A}x_{1A}}(\pm t_1)|$ in Fig. 4(b) also manifest the skin effect, which is algebraically divergent with L [64,77].

The above signature for detecting the coexisting topological phase (i.e., the zero-frequency dip) will be destroyed by the dissipation or perturbation of the system. Figures 4(c) and 4(d) show that the dip of $|S_{x_{1A}x_{1A}}(0)|$ disappears at the critical point $\gamma_c \equiv \sqrt{g_2^2 - (t_1 - t_2)^2}$ (see Supplemental Material [77]). Physically, the presence of dissipation moves the effective spectrum to the lower half plane, and the reference frequency ω would go out of the loop as increasing γ. Figure 4(e) demonstrates that the zero-frequency dip vanishes at the scaling $\mu/t_1 \sim \xi^{-L}$, since the perturbation breaks the time-reversal symmetry.

Conclusion.—We have shown the squeezing-induced point-gap topology together with the $\mathbb{Z}_2$ skin effect in the QBS, when time-reversal symmetry is introduced. The interplay of the bosonic squeezing and particle-exchange coupling results in the survival of zero modes in the OBC even if a real gap closes in the PBC. This exhibits an anomalous bulk-boundary correspondence. Our Letter enriches non-Bloch topological physics in the QBS by predicting the real- and point-gap coexisting topological phase. This may stimulate future studies of symmetry-enriched topological physics in the higher-dimensional systems. Our Letter also provides a perfect example of the combination of nonlinearity and non-Hermiticity with topology, and it will inspire experimental activity in the field of nonlinear topological photonics [102].

L.-L. W. is very thankful to Dr. Zixian Zhou for his fruitful discussions. This work is supported by the National Key Research and Development Program of China (Grant No. 2021YFA1400700), the National Natural Science Foundation of China (Grants No. 11974125, No. 12205109, and No. 12147143).

*xinyoulu@hust.edu.cn

[1] T. Ozawa, H. M. Price, A. Amo, N. Goldman, M. Hafezi, L. Lu, M. C. Rechtsman, D. Schuster, J. Simon, O. Zilberberg, and I. Carusotto, Rev. Mod. Phys. **91**, 015006 (2019).
[2] D. Jin, L. Lu, Z. Wang, C. Fang, J. D. Joannopoulos, M. Soljačić, L. Fu, and N. X. Fang, Nat. Commun. **7**, 13486 (2016).
[3] L. M. Nash, D. Kleckner, A. Read, V. Vitelli, A. M. Turner, and W. T. M. Irvine, Proc. Natl. Acad. Sci. U.S.A. **112**, 14495 (2015).
[4] Z. Yang, F. Gao, X. Shi, X. Lin, Z. Gao, Y. Chong, and B. Zhang, Phys. Rev. Lett. **114**, 114301 (2015).
[5] S. D. Huber, Nat. Phys. **12**, 621 (2016).
[6] M.-J. Tuo, L.-H. Zhang, D. Liu, R.-W. Peng, R.-H. Fan, Z.-G. Chen, Y. Wu, D.-X. Qi, and M. Wang, Phys. Rev. B **99**, 205432 (2019).
[7] D.-W. Zhang, Y.-Q. Zhu, Y. X. Zhao, H. Yan, and S.-L. Zhu, Adv. Phys. **67**, 253 (2018).
[8] N. R. Cooper, J. Dalibard, and I. B. Spielman, Rev. Mod. Phys. **91**, 015005 (2019).
[9] T. Phan, D. Sell, E. W. Wang, S. Doshay, K. Edee, J. Yang, and J. A. Fan, Light Sci. Appl. **8**, 48 (2019).
[10] Y.-J. Gao, X. Xiong, Z. Wang, F. Chen, R.-W. Peng, and M. Wang, Phys. Rev. X **10**, 031035 (2020).
[11] Q. Song, M. Odeh, J. Zúñiga-Pérez, B. Kanté, and P. Genevet, Science **373**, 1133 (2021).
[12] M. S. Rudner and L. S. Levitov, Phys. Rev. Lett. **102**, 065703 (2009).
[13] K. Esaki, M. Sato, K. Hasebe, and M. Kohmoto, Phys. Rev. B **84**, 205128 (2011).
[14] T. E. Lee, Phys. Rev. Lett. **116**, 133903 (2016).
[15] D. Leykam, K. Y. Bliokh, C. Huang, Y. D. Chong, and F. Nori, Phys. Rev. Lett. **118**, 040401 (2017).
[16] Y. Xu, S.-T. Wang, and L.-M. Duan, Phys. Rev. Lett. **118**, 045701 (2017).
[17] H. Shen, B. Zhen, and L. Fu, Phys. Rev. Lett. **120**, 146402 (2018).
[18] S. Yao and Z. Wang, Phys. Rev. Lett. **121**, 086803 (2018).
[19] Z. Gong, Y. Ashida, K. Kawabata, K. Takasan, S. Higashikawa, and M. Ueda, Phys. Rev. X **8**, 031079 (2018).
[20] F. K. Kunst, E. Edvardsson, J. C. Budich, and E. J. Bergholtz, Phys. Rev. Lett. **121**, 026808 (2018).
[21] H. Zhou and J. Y. Lee, Phys. Rev. B **99**, 235112 (2019).
[22] D. Porras and S. Fernández-Lorenzo, Phys. Rev. Lett. **122**, 143901 (2019).
[23] K. Kawabata, K. Shiozaki, M. Ueda, and M. Sato, Phys. Rev. X **9**, 041015 (2019).
[24] C. H. Lee and R. Thomale, Phys. Rev. B **99**, 201103(R) (2019).

[25] K. Yokomizo and S. Murakami, Phys. Rev. Lett. **123**, 066404 (2019).
[26] N. Okuma and M. Sato, Phys. Rev. Lett. **123**, 097701 (2019).
[27] F. Song, S. Yao, and Z. Wang, Phys. Rev. Lett. **123**, 170401 (2019).
[28] Z. Yang, K. Zhang, C. Fang, and J. Hu, Phys. Rev. Lett. **125**, 226402 (2020).
[29] D. S. Borgnia, A. J. Kruchkov, and R.-J. Slager, Phys. Rev. Lett. **124**, 056802 (2020).
[30] N. Okuma, K. Kawabata, K. Shiozaki, and M. Sato, Phys. Rev. Lett. **124**, 086801 (2020).
[31] K. Zhang, Z. Yang, and C. Fang, Phys. Rev. Lett. **125**, 126402 (2020).
[32] K. Zhang, Z. Yang, and C. Fang, Nat. Commun. **13**, 2496 (2022).
[33] S. Longhi, Phys. Rev. Lett. **128**, 157601 (2022).
[34] B. Zhu, Q. Wang, D. Leykam, H. Xue, Q. J. Wang, and Y. D. Chong, Phys. Rev. Lett. **129**, 013903 (2022).
[35] H. Zhao, X. Qiao, T. Wu, B. Midya, S. Longhi, and L. Feng, Science **365**, 1163 (2019).
[36] T. Helbig, T. Hofmann, S. Imhof, M. Abdelghany, T. Kiessling, L. W. Molenkamp, C. H. Lee, A. Szameit, M. Greiter, and R. Thomale, Nat. Phys. **16**, 747 (2020).
[37] L. Xiao, T. Deng, K. Wang, G. Zhu, Z. Wang, W. Yi, and P. Xue, Nat. Phys. **16**, 761 (2020).
[38] A. Ghatak, M. Brandenbourger, J. van Wezel, and C. Coulais, Proc. Natl. Acad. Sci. U.S.A. **117**, 29561 (2020).
[39] T. Hofmann, T. Helbig, F. Schindler, N. Salgo, M. Brzezińska, M. Greiter, T. Kiessling, D. Wolf, A. Vollhardt, A. Kabaši, C. H. Lee, A. Bilušić, R. Thomale, and T. Neupert, Phys. Rev. Res. **2**, 023265 (2020).
[40] S. Weidemann, M. Kremer, T. Helbig, T. Hofmann, A. Stegmaier, M. Greiter, R. Thomale, and A. Szameit, Science **368**, 311 (2020).
[41] F. E. Öztürk, T. Lappe, G. Hellmann, J. Schmitt, J. Klaers, F. Vewinger, J. Kroha, and M. Weitz, Science **372**, 88 (2021).
[42] K. Wang, A. Dutt, K. Y. Yang, C. C. Wojcik, J. Vučković, and S. Fan, Science **371**, 1240 (2021).
[43] Q. Liang, D. Xie, Z. Dong, H. Li, H. Li, B. Gadway, W. Yi, and B. Yan, Phys. Rev. Lett. **129**, 070401 (2022).
[44] S. L. Braunstein and P. van Loock, Rev. Mod. Phys. **77**, 513 (2005).
[45] X.-Y. Lü, Y. Wu, J. R. Johansson, H. Jing, J. Zhang, and F. Nori, Phys. Rev. Lett. **114**, 093602 (2015).
[46] W. Qin, A. Miranowicz, P.-B. Li, X.-Y. Lü, J. Q. You, and F. Nori, Phys. Rev. Lett. **120**, 093601 (2018).
[47] C. Leroux, L. C. G. Govia, and A. A. Clerk, Phys. Rev. Lett. **120**, 093602 (2018).
[48] W. Ge, B. C. Sawyer, J. W. Britton, K. Jacobs, J. J. Bollinger, and M. Foss-Feig, Phys. Rev. Lett. **122**, 030501 (2019).
[49] W. Zhao, S.-D. Zhang, A. Miranowicz, and H. Jing, Sci. China Phys. Mech. Astron. **63**, 224211 (2019).
[50] C. J. Zhu, L. L. Ping, Y. P. Yang, and G. S. Agarwal, Phys. Rev. Lett. **124**, 073602 (2020).
[51] Y.-H. Chen, W. Qin, X. Wang, A. Miranowicz, and F. Nori, Phys. Rev. Lett. **126**, 023602 (2021).
[52] W. Qin, A. Miranowicz, H. Jing, and F. Nori, Phys. Rev. Lett. **127**, 093602 (2021).
[53] R. Barnett, Phys. Rev. A **88**, 063631 (2013).
[54] B. Galilo, D. K. K. Lee, and R. Barnett, Phys. Rev. Lett. **115**, 245302 (2015).
[55] G. Engelhardt, M. Benito, G. Platero, and T. Brandes, Phys. Rev. Lett. **117**, 045302 (2016).
[56] V. Peano, M. Houde, F. Marquardt, and A. A. Clerk, Phys. Rev. X **6**, 041026 (2016).
[57] D. Malz, J. Knolle, and A. Nunnenkamp, Nat. Commun. **10**, 3937 (2019).
[58] Y. Ashida, Z. Gong, and M. Ueda, Adv. Phys. **69**, 249 (2020).
[59] E. J. Bergholtz, J. C. Budich, and F. K. Kunst, Rev. Mod. Phys. **93**, 015005 (2021).
[60] D. Bernard and A. LeClair, A classification of non-Hermitian random matrices, in *Statistical Field Theories*, edited by A. Cappelli and G. Mussardo (Springer Netherlands, Dordrecht, 2002), pp. 207–214.
[61] A. McDonald, T. Pereg-Barnea, and A. A. Clerk, Phys. Rev. X **8**, 041031 (2018).
[62] C. C. Wanjura, M. Brunelli, and A. Nunnenkamp, Nat. Commun. **11**, 3149 (2020).
[63] V. P. Flynn, E. Cobanera, and L. Viola, New J. Phys. **22**, 083004 (2020).
[64] V. P. Flynn, E. Cobanera, and L. Viola, Phys. Rev. Lett. **127**, 245701 (2021).
[65] Q. Wang, C. Zhu, Y. Wang, B. Zhang, and Y. D. Chong, Phys. Rev. B **106**, 024301 (2022).
[66] Á. Gómez-León, T. Ramos, A. González-Tudela, and D. Porras, arXiv:2207.13715.
[67] N. Hatano and D. R. Nelson, Phys. Rev. Lett. **77**, 570 (1996).
[68] N. Hatano and D. R. Nelson, Phys. Rev. B **56**, 8651 (1997).
[69] K. Yokomizo and S. Murakami, Phys. Rev. B **103**, 165123 (2021).
[70] R. Rossignoli and A. M. Kowalski, Phys. Rev. A **72**, 032101 (2005).
[71] L. R. Israel Gohberg and Peter Lancaster, *Indefinite Linear Algebra and Applications* (Birkhäuser, Basel, 2005).
[72] C.-E. Bardyn, T. Karzig, G. Refael, and T. C. H. Liew, Phys. Rev. B **93**, 020502(R) (2016).
[73] V. Peano, M. Houde, C. Brendel, F. Marquardt, and A. A. Clerk, Nat. Commun. **7**, 10779 (2016).
[74] S. Lieu, Phys. Rev. B **98**, 115135 (2018).
[75] A. Mostafazadeh, J. Math. Phys. (N.Y.) **43**, 205 (2001).
[76] N. Okuma, Phys. Rev. B **105**, 224301 (2022).
[77] See Supplemental Material at http://link.aps.org/supplemental/10.1103/PhysRevLett.130.203605 for proofs of some claims and technical details on the considered system, which includes Refs. [76–83].
[78] A. Kitaev, AIP Conf. Proc. **1134**, 22 (2009).
[79] C.-K. Chiu, J. C. Y. Teo, A. P. Schnyder, and S. Ryu, Rev. Mod. Phys. **88**, 035005 (2016).
[80] L.-L. Wan, Z. Zhou, and Z.-F. Xu, Phys. Rev. A **103**, 013308 (2021).
[81] C. Gardiner and P. Zoller, *Quantum Noise* (Springer, Berlin, Heidelberg, 2004).
[82] D. C. Brody, J. Phys. A **47**, 035305 (2013).
[83] J. Williamson, Am. J. Math. **58**, 141 (1936).
[84] R. Simon, S. Chaturvedi, and V. Srinivasan, J. Math. Phys. (N.Y.) **40**, 3632 (1999).

[85] A. I. Lvovsky, *Squeezed Light. In Photonics*, edited by D. L. Andrews (Wiley, New York, 2015), Chap. 5.
[86] B. Abdo, A. Kamal, and M. Devoret, Phys. Rev. B **87**, 014508 (2013).
[87] M. Fitzpatrick, N. M. Sundaresan, A. C. Y. Li, J. Koch, and A. A. Houck, Phys. Rev. X **7**, 011016 (2017).
[88] N. E. Frattini, U. Vool, S. Shankar, A. Narla, K. M. Sliwa, and M. H. Devoret, Appl. Phys. Lett. **110**, 222603 (2017).
[89] P. Krantz, M. Kjaergaard, F. Yan, T. P. Orlando, S. Gustavsson, and W. D. Oliver, Appl. Phys. Rev. **6**, 021318 (2019).
[90] C. S. Wang, J. C. Curtis, B. J. Lester, Y. Zhang, Y. Y. Gao, J. Freeze, V. S. Batista, P. H. Vaccaro, I. L. Chuang, L. Frunzio, L. Jiang, S. M. Girvin, and R. J. Schoelkopf, Phys. Rev. X **10**, 021060 (2020).
[91] D. W. C. Brooks, T. Botter, S. Schreppler, T. P. Purdy, N. Brahms, and D. M. Stamper-Kurn, Nature (London) **488**, 476 (2012).
[92] A. H. Safavi-Naeini, S. Gröblacher, J. T. Hill, J. Chan, M. Aspelmeyer, and O. Painter, Nature (London) **500**, 185 (2013).
[93] J. del Pino, J. J. Slim, and E. Verhagen, Nature (London) **606**, 82 (2022).
[94] M. Sato, K. Hasebe, K. Esaki, and M. Kohmoto, Prog. Theor. Phys. **127**, 937 (2012).
[95] S. Lieu, M. McGinley, and N. R. Cooper, Phys. Rev. Lett. **124**, 040401 (2020).
[96] N. Okuma and M. Sato, Phys. Rev. B **102**, 014203 (2020).
[97] K. Kawabata, N. Okuma, and M. Sato, Phys. Rev. B **101**, 195147 (2020).
[98] Squeezing transformation is unitary in the second-quantization langauge, but becomes a pseudounitary matrix in the first-quantization langauge, which acts on an indefinite Hilbert space with metric τ^3 [71,75,77].
[99] Here the continuum limit refers to the fact that both ends of the chain go to infinity, which is the so-called infinite boundary condition. One should not be confused with the semi-infinite boundary condition [19,30]. Moreover, the infinite boundary condition is equivalent to the PBC by taking $L \to \infty$ [100].
[100] L. N. Trefethen and M. Embree, *Spectra and Pseudospectra: The Behavior of Nonnormal Matrices and Operators* (Princeton University Press, Princeton, NJ, 2005).
[101] L. Li, C. H. Lee, S. Mu, and J. Gong, Nat. Commun. **11**, 5491 (2020).
[102] D. Smirnova, D. Leykam, Y. Chong, and Y. Kivshar, Appl. Phys. Rev. **7**, 021306 (2020).